Assessment and Comparison of Multicarrier Waveforms Under Nonlinear Conditions

Kiril Kirev*, Stefan Schwarz†
†Christian Doppler Laboratory for Dependable Wireless Connectivity for the Society in Motion
*†TU Wien, Institute of Telecommunications
Gusshausstrasse 25/389, A-1040 Vienna, Austria
*Email: kiril.kirev@tuwien.ac.at
†Email: sschwarz@nt.tuwien.ac.at

***Abstract*—Power Amplifiers (PAs) are inherently nonlinear devices for which power efficiency and amplifier linearity are a trade-off recourse. On the one hand, poor power efficiency reduces the battery life of a mobile device, or is accompanied by a significant financial burden in the case of a base station. On the other hand, driving the amplifier above the linear regime to increase power efficiency distorts the amplified signal in a nonlinear fashion. This distortion not only deteriorates the transmission quality, but also introduces interference in adjacent frequency channels. Multicarrier systems, in which the signal bandwidth is shared among multiple pulses, are particularly vulnerable to Out-Of-Band (OOB) interference. Robustness against such interferences caused by nonlinear amplification is to be considered when choosing the right modulation scheme. In this paper, the following modulation waveforms are compared: OFDM, FOFDM, WOLA, UFMC, FBMC-OQAM and Pruned DFT-Spread FBMC, and their sensitivity towards nonlinear distortions is assessed. For this purpose, the Vienna 5G Link Level Simulator is used, which allows for a fair comparison of the waveforms on a unified platform.**

***Index Terms*—Power Amplifiers, Nonlinearity, SIR, PAPR, OFDM, FBMC, Simulation**

I. Introduction

As the demand for higher data rate connectivity increases, mobile networks tend to increase the bandwidth, to go to higher carrier frequency and to utilize multi-pulse modulations with nonconstant amplitudes to achieve higher spectral efficiency. These requirements pose a challenge on the transmit Power Amplifier (PA). On the one hand, the PA's output signal for small input values follows the amplifier gain linearly and deteriorates with increasing drive level, manifesting in unwanted frequencies in adjacent channels, known as Intermodulation Products (IC) and output signal power saturation. On the other hand, the amplifier can be a main source of power consumption in communication systems and thus defining the battery life for mobile devices. Thus, a trade-off between the device's power efficiency and its distortion level arises. In this paper, the effects of this trade-off under different modulation waveforms are examined. Even though the 3rd Generation Partnership Project (3GPP) decided to stay with OFDM as the preferred waveform for 5G [14], it is still worthwhile to perform this comparative study, as OFDM is not the most efficient modulation in all use cases. The goal is to evaluate the robustness of different modulation waveforms against nonlinear distortions under the unified platform of the Vienna 5G Link-Level Simulator [5]. For this purpose, the following metrics will be considered: Signal-to-Interference Ratio (SIR) as a measure for Out-of-Band (OOB) emissions, Peak-to-Average Power Ratio (PAPR) as a measure for the complex signal envelope variation, and Bit Error Ratio (BER) as a measure for the transmission quality. The structure of this paper is as follows: Sec. II gives a brief introduction in PA design and how it affects their nonlinear characteristic. It also includes a description of the system model used for parametrisation of said characteristic. Sec. III introduces multicarrier waveforms in a brief manner. Sec. IV discusses simulation procedures and results. The paper summary follows finally in Sec. V.

II. Power Amplifier Model

There are two dominant technologies when it comes to microwave PA design, namely the Travelling-Wave-Tube Amplifiers (TWTA) and Solid-State Power Amplifiers (SSPA). While TWTAs were once the preferred choice, their area of use nowadays is mostly in satellite, broadcasting and radar communication systems. Meanwhile, advancements in Integrated Circuits (IC) allow the design of SSPAs with high output power, prolonged operational time, higher modulation frequency, robust design and compact size. This allows for their implementation not only in hand-held devices, but also in base stations, broadcasting and satellite communications [1]. The two technologies have a somewhat different amplification behaviour that has to be taken into consideration when choosing a model. Another vital point is the memory effects PAs exhibit, that is the dependence of the output signal in a current instance on the output signal in previous instances [2]. When the bandwidth of the signal is small, relative to the carrier frequency, it is said to be a narrow-band channel [3]

$$B_s \ll f_c, \tag{1}$$

where B_s is the bandwidth of the bandpass signal $s(t)$ and f_c its carrier frequency. Under this condition, we can simplify the model by assuming a memoryless system, expressed in the drop of time-dependency in $s(t)$. At this point it is worth introducing the equivalent baseband representation s_b of the bandpass signal s, which can be expressed as

$$s_b = u_s e^{j\alpha_s}, \tag{2}$$

with u_s being the amplitude and α_s being the phase of the signal . Then the equivalence can be formulated as follows

$$s = \mathrm{Re}\{s_b e^{j2\pi f_c}\} = \frac{1}{2} s_b e^{j2\pi f_c} + \frac{1}{2} s_b^* e^{-j2\pi f_c}. \tag{3}$$

Then, the baseband modelling of a memoryless, nonlinear PA system can be expressed as

$$y_b = G(u_s) e^{j(\alpha_s + \Phi(u_s))}, \tag{4}$$

where $G(u_s)$ is the conversion from input amplitude to output amplitude, called Amplitude Modulation to Amplitude Modulation (AM/AM) and $\Phi(u_s)$ the conversion from input amplitude to output phase, called Amplitude Modulation to Phase Modulation (AM/PM). Notice that both functions depend solely on the input amplitude (signal envelope).
Under these considerations, the model chosen for this work is the Rapp model [4]. It is used to model memoryless nonlinearities in SSPAs in complex baseband representation and its AM/AM and AM/PM functions are the following

$$G(u_s) = \frac{V u_s}{\left[1 + \left(\frac{V u_s}{u_{s,sat}}\right)^{2p}\right]^{\frac{1}{2p}}}, \tag{5}$$

$$\Phi(u_s) = 0, \tag{6}$$

where p is a smoothness factor, V the small signal amplification of the PA and $u_{s,sat}$ the saturation amplitude of the output signal. Notice that since the phase is not affected by the model, it represents a true memoryless system. Fig. 1 shows the model characteristic function with values $p = 3$, $V = 1$ and $u_{s,sat} = 1$, which associates the relative output power as a function of the relative input power.

A. Amplifier Quiescent Point

The quiescent point of an amplifier is commonly referred to as setting the operating currents or voltages of a device in the absence of input signals [6]. A common way to define this point is by the Output-Back-Off (OBO) of a PA [7], which is the logarithmic ratio between output saturation power, $P_{max,out}$, and mean output power, σ_y^2

$$\mathrm{OBO} = 10 \log_{10}\Big(\frac{P_{max,out}}{\sigma_y^2}\Big). \tag{7}$$

Using this definition, one can express the saturation amplitude of the amplifier's output signal, $u_{s,sat}$, as a function of its OBO

$$u_{s,sat} = \sigma_y 10^{\frac{\mathrm{OBO}}{20}}. \tag{8}$$

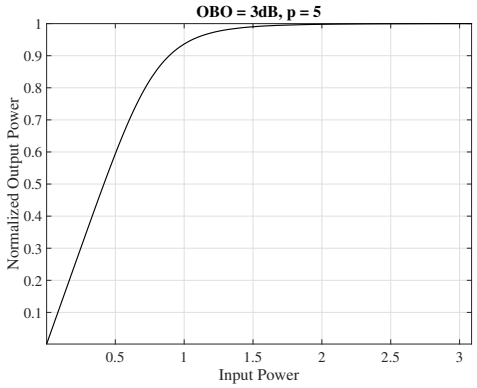

Fig. 1. AM/AM characteristic function of the Rapp model

The OBO value is directly related to the amplifier's linearity profile and power efficiency. High OBO values translate to operating in the PA's linear regime, but also mean low power efficiency, and vice versa, making it a suitable model parameter.

B. Peak-to-Average Power Ratio

The PAPR is defined as

$$\mathrm{PAPR}(\mathbf{s}(t)) = \frac{\max\limits_{0 \le t \le K T_s} |s(t)|^2}{\mathbb{E}\{|s(t)|^2\}}, \tag{9}$$

where K denotes the number of symbols and T_s denotes the transmission period per symbol, and serves as a measure for the impulsiveness of the signal. High PAPR values correspond not only to increased linearity requirements for the PAs, but also to higher resolution requirements for the Digital-to-Analog converters (DAC) at the transmission equipment, both of which lead to reduced power efficiency.

III. Modulation Waveforms

All modulation waveforms considered in this paper are implementations of multicarrier systems, which utilize orthogonal pulses that overlap in frequency and time. The basic concept is to split the transmitted signal, which generally has a wider bandwidth than a single pulse, into many different subchannels so that effectively each of them experiences flat fading, relative to the complete frequency-selective channel and thus reducing the Intersymbol Interference (ISI) [12]. The mathematical expression for the modulated signal is

$$s(t) = \sum_{k=-\infty}^{+\infty} \sum_{n=0}^{N-1} x_{k,n} h_{k,n}(t), \tag{10}$$

where $x_{k,n}$ denotes the data symbol at the k^{th} time position and the n^{th} subcacarrier position, and the variable $h_{k,n}(t)$ denotes the transmitted basis pulse. One possible definition of said pulse can be expressed as

$$h_{k,n}(t) = p_{TX}(t - kT) e^{j2\pi n F (t - kT)} e^{j\theta_{k,n}}, \tag{11}$$

TABLE I
PROTOTYPE FILTER LIST

Modulation	Filter/Windowing function	Symbol Density TF	Transmission Duration
OFDM	Rectangular	1.07	1ms
FOFDM	Rectangular, soft-truncated Hann window	1.07	1ms
WOLA	Root-Raised Cosine	1.07	1ms
UFMC	Dolph-Chebyshev	1.07	1ms
FBMC-OQAM	PHYDYAS [13]	1	1ms
Pruned DFT-Spread FBMC	Truncated Hermite	1	1ms

with $p_{TX}(t)$ denoting the transmit prototype filter, T the time spacing, F the frequency(subcarrier) spacing and $\theta_{k,n}$ a phase shift [15]. On reception, the transmitted symbols are then reconstructed by projecting the received signal, $r(t)$, onto the receive basis pulses, $g_{k,n}(t)$, so that

$$y_{k,n} = \int_{-\infty}^{\infty} r(t) g_{k,n}^{*}(t) \mathrm{d}t. \tag{12}$$

These basis pulses are defined analogously to (11) as

$$g_{k,n}(t) = p_{RX}(t - kT) e^{j2\pi nF(t-kT)} e^{j\theta_{k,n}}, \tag{13}$$

the only difference being the receive prototype filter $p_{RX}(t)$. One of the main differences between these multicarrier systems is the applied filter granularity. In classical OFDM, filtering is done on the whole band. While simple in design and in implementation, rectangular time pulses have poor spectral properties, expressed in the slowly decaying side lobes of the signals Power Spectral Density (PSD), resulting in increase in OOB emissions. One way of suppressing the spectral leakage is to smoothen the filter edges by applying a windowing function, as done in WOLA [17]. A similar approach is to apply filtering on a subband level instead of on the whole band. Such an approach is used by f-OFDM [10] and UFMC [11]. In contrast, FBMC employs filtering on a subcarrier level. There are different definitions of FMBC in the literature [18]–[20], differentiating in the way they satisfy the Balian-Low design constraint, but we chose the construction method in [15] in combination with Offset Quadrature Amplitude Modulation (OQAM) [8] as it matches our design goals of OOB reduction and enhanced spectral efficiency. It also allows for a simple construction of the final multicarrier system considered in this paper, the Pruned DFT-Spread FBMC [9], achieved by applying a spreading transformation in frequency on the basis pulses, $g_{k,n}$, effectively setting half of them to zero.

From (10)-(13) it becomes apparent that the primary characteristics of multicarrier systems are the subcarrier and time spacing, F and T, as well as the prototype filters, p_{TX} and p_{RX}. The product of the former two parameters is called symbol density, $TF \geqslant 1$, and is inversely proportional to the spectral efficiency. According to the Balian-Low theorem [16], there exists a fundamental constraint in the design of multicarrier systems such that it is mathematically impossible to fulfill all desired properties of the system, which includes orthogonality of the basis pulses in frequency and time. In order to do a fair comparison between the different modulation waveforms, we sacrifice orthogonality in WOLA, FOFDM and UFMC to achieve the same spectral efficiency as OFDM. [21]. The choice of the latter two of the characterizing parameters depends on the transmission conditions. One could set them either identically, thus $g_{k,n}(t) = h_{k,n}(t)$, or have different p_{TX} and p_{RX} filters. Throughout this paper, identical transmit and receive filters are considered, the only exception being OFDM, where due to the presence of a Cyclic Prefix (CP) different filter lengths are used. Table I lists the chosen filters, together with the corresponding symbol density and overall transmission duration.

TABLE II
SIMULATION PARAMETERS

Channel model:	Rayleigh Fading
Power Delay Profile:	Pedastrian A [22]
Modulation alphabet:	64QAM
Monte Carlo repetitions:	5000
Channel Coding:	Uncoded
System bandwidth:	0.72MHz
Guard Band:	0.144MHz
Subcarrier spacing:	15kHz
Number of subcarriers:	48
Number of sumbols:	14
Payload (bits):	6216
FFT Size:	336
Rapp model parameters	
Smoothness factor:	5
OBO:	3dB

IV. RESULTS

This section presents the simulation results with the main parameters summarized in Table II. A frequency-selective channel was chosen together with a predefined Power Delay Profile (PDP), here 3GPPs Pedestrian A, and is included only in the BER calculation. Fig. 2 shows the PSD affected by the amplifier nonlinearity. It is clear that the superior spectral properties of both FBMC schemes, as well as the filtered/windowed OFDM schemes, are negated by the amplifiers clipping effect, making them comparable to CP-OFDM.

The Complementary Cumulative Distribution Function (CCDF) of the different PAPR values, together with a reference result for a single carrier system (we chose SC-FDMA), are shown in fig. 3. The majority of the underlying multicarrier systems produce similarly high PAPR values due to the number of added basis pulses, together with the central limit theorem. On the contrary, the pruned FBMC system's

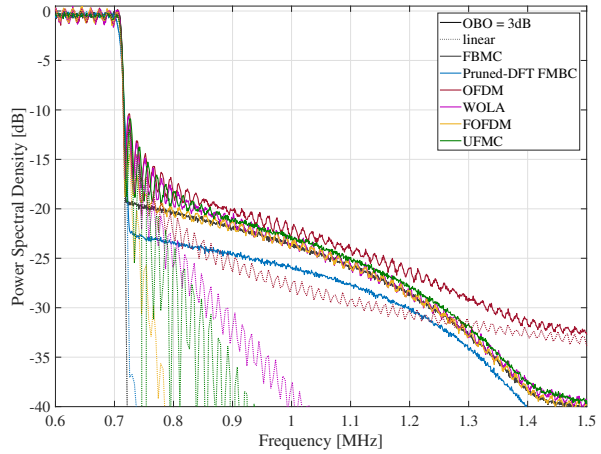

Fig. 2. Power spectral density, with and without nonlinearity

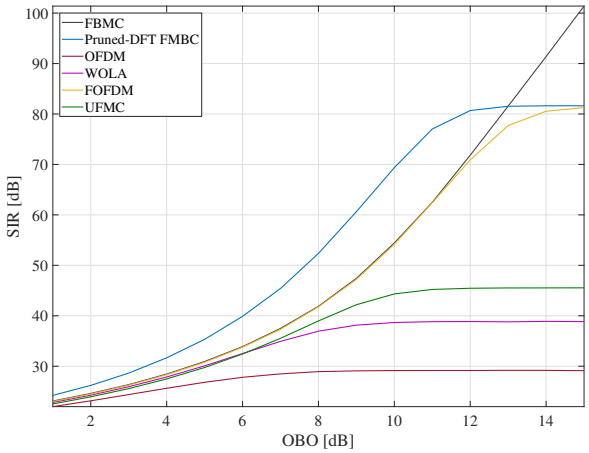

Fig. 5. Signal-to-Interference ratio for different OBO values

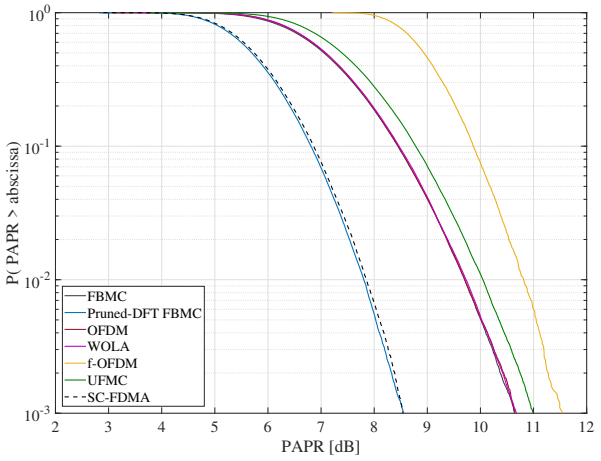

Fig. 3. Peak-to-Average Power Ratio of the different modulation waveforms

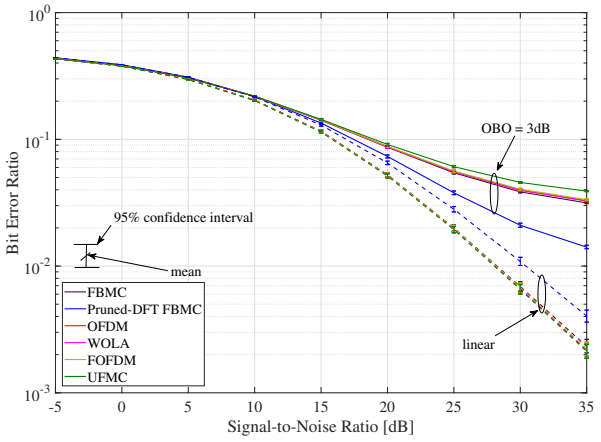

Fig. 4. Bit Error Ratio, with and without nonlinearity

performance resembles that of a single-carrier system, due to reduction of the number of basis pulses and spreading them in frequency, which leads to smoothing of the signal.

Fig. 4 shows the BER with and without the inclusion of a PA nonlinearity. With the chosen modulation parameters, the pruned FBMC performs around $3dB$ worse than the other waveforms without considering the nonlinear amplifier. It does, however, show the most resilience against nonlinear distortions.

For the SIR calculation we assume the following scenario: Two users within the same band, each being allocated $N = 48$ subcarriers and $K = 14$ symbols, resulting in a bandwidth $BW = 0.72$MHz, are separated by a guard band of $F_G = 0.144$MHz. We consider interference in the useful bandwidth of the first user, caused by the presence of the second user, and define it as

$$\text{SIR} = \frac{\sum_{f \in BW_{Ch1}} |S_S(f)|^2}{\sum_{f \in BW_{Ch1}} |S_I(f)|^2}, \tag{14}$$

where $S_S(f)$ is the Fourier transform of the first user's signal, $S_I(f)$ the Fourier transform of the second user's signal, and BW represents the transmission band associated with the first user. We consider the sum interference power, although subcarriers that are nearest to the other user will be the most affected. Simulation results are shown in fig. 5 as a function of the amplifier's OBO. It should be noted that the SIR calculation is somewhat simplified, as we ignored channel statistics, different receive power levels, self-caused interference, and have concentrated on effects caused mainly by spectral leakage.

V. Summary

In this paper, multiple modulation waveforms were compared and their robustness towards amplifier nonlinearities was evaluated. A pruned version of FBMC showed to be most prominent, indicated by single-carrier comparable PAPR values, as well as by the BER and SIR results under nonlinear

conditions. It does, however, suffer from a performance loss due to spreading under linear conditions.

As our work is purely simulation-based, it serves more as a guideline on how the different multicarrier systems are affected by nonlinearities compared to one another on a unifying platform. Real-life experiments are needed especially for the SIR calculation, where a lot of realistic conditions were left out.

VI. Acknowledgements

The financial support by the Austrian Federal Ministry for Digital and Economic Affairs and the National Foundation for Research, Technology and Development is gratefully acknowledged.

References

[1] Theeuwen, S. J. C. H., and J. H. Qureshi. "LDMOS technology for RF power amplifiers." IEEE transactions on microwave theory and techniques 60.6 (2012): 1755-1763.APA

[2] Vuolevi, Joel HK, Timo Rahkonen, and Jani PA Manninen. "Measurement technique for characterizing memory effects in RF power amplifiers." IEEE Transactions on microwave theory and techniques 49.8 (2001): 1383-1389.

[3] Molisch, Andreas F. Wireless communications. Vol. 34. John Wiley & Sons, 2012.

[4] Rapp, Christoph. "Effects of HPA-nonlinearity on a 4-DPSK/OFDM-signal for a digital sound broadcasting signal." In ESA, Second European Conference on Satellite Communications (ECSC-2) p 179-184 (SEE N92-15210 06-32). 1991.

[5] Pratschner, Stefan, et al. "Versatile mobile communications simulation: The Vienna 5G link level simulator." EURASIP Journal on Wireless Communications and Networking 2018.1 (2018): 226.

[6] Horowitz, Paul, and Winfield Hill. The art of electronics. Cambridge Univ. Press, 1989.

[7] Deumal, Marc. "Multicarrier communication systems with low sensitivity to nonlinear amplification." Enginyeria i Arquitectura La Salle, Universitat Ramon Llull, Barcelona (2008).

[8] Bölcskei, Helmut. "Orthogonal frequency division multiplexing based on offset QAM." Advances in Gabor analysis. Birkhäuser, Boston, MA, 2003. 321-352.

[9] Nissel, Ronald, and Markus Rupp. "Pruned DFT Spread FBMC: Low PAPR, Low Latency, High Spectral Efficiency." IEEE Transactions on Communications (2018).

[10] Zhang, Xi, et al. "Filtered-OFDM-enabler for flexible waveform in the 5th generation cellular networks." 2015 IEEE Global Communications Conference (GLOBECOM). IEEE, 2015.

[11] Vakilian, Vida, et al. "Universal-filtered multi-carrier technique for wireless systems beyond LTE." 2013 IEEE Globecom Workshops (GC Wkshps). IEEE, 2013.

[12] Goldsmith, Andrea. Wireless communications. Cambridge university press, 2005.

[13] M. Bellanger, D. Le Ruyet, D. Roviras, M. Terr, J. Nossek, L. Baltar, Q. Bai, D. Waldhauser, M. Renfors, T. Ihalainen, et al., FBMC physical layer: a primer, PHYDYAS, January, 2010.

[14] 3GPP, TSG RAN; study on new radio access technology; radio interface protocol aspects; (release 14). http://www.3gpp.org/DynaReport/38804.htm, Mar. 2017.

[15] Nissel, Ronald, Stefan Schwarz, and Markus Rupp. "Filter bank multicarrier modulation schemes for future mobile communications." IEEE Journal on Selected Areas in Communications 35.8 (2017): 1768-1782.

[16] Benedetto, John J., Christopher Heil, and David F. Walnut. "Gabor systems and the Balian-Low theorem." Gabor analysis and algorithms. Birkhäuser, Boston, MA, 1998. 85-122.

[17] Sahin, Alphan, and Huseyin Arslan. "Edge windowing for OFDM based systems." IEEE Communications Letters 15.11 (2011): 1208-1211.

[18] Nam, Hyungju, et al. "A new filter-bank multicarrier system with two prototype filters for QAM symbols transmission and reception." IEEE Transactions on Wireless Communications 15.9 (2016): 5998-6009.

[19] Schaich, Frank. "Filterbank based multi carrier transmission (FBMC)evolving OFDM: FBMC in the context of WiMAX." 2010 European Wireless Conference (EW). IEEE, 2010.

[20] Kim, Chanhong, et al. "Introduction to QAM-FBMC: From waveform optimization to system design." IEEE Communications Magazine 54.11 (2016): 66-73.

[21] Gerzaguet, Robin, et al. "The 5G candidate waveform race: a comparison of complexity and performance." EURASIP Journal on Wireless Communications and Networking 2017.1 (2017): 13.

[22] 3rd Generation Partnership Project (3GPP). Technical Speci
cation Group Radio Access Network; High Speed Downlink Packet Access: UE Radio Transmission and Reception. TR 25.890. 3rd Generation Partnership Project (3GPP), May 2002.